Harmful Algae 54 (2016) 160–173

Contents lists available at ScienceDirect

Harmful Algae

journal homepage: www.elsevier.com/locate/hal

Review

Challenges for mapping cyanotoxin patterns from remote sensing of cyanobacteria

Richard P. Stumpf [a,*], Timothy W. Davis [b], Timothy T. Wynne [a], Jennifer L. Graham [c], Keith A. Loftin [c], Thomas H. Johengen [d], Duane Gossiaux [b], Danna Palladino [d], Ashley Burtner [d]

[a] National Oceanic and Atmospheric Administration, National Centers for Coastal Ocean Science, Silver Spring, MD, USA
[b] National Oceanic and Atmospheric Administration, Great Lakes Environmental Research Laboratory, Ann Arbor, MI, USA
[c] United States Geological Survey, Kansas Water Science Center, Lawrence, KS, USA
[d] Cooperative Institute for Limnology & Ecosystem Research (CILER), Ann Arbor, MI, USA

ARTICLE INFO

Article history:
Received 30 September 2015
Received in revised form 14 January 2016
Accepted 15 January 2016

Keywords:
Microcystins
Satellite
MERIS
Chlorophyll
Phycocyanin

ABSTRACT

Using satellite imagery to quantify the spatial patterns of cyanobacterial toxins has several challenges. These challenges include the need for surrogate pigments – since cyanotoxins cannot be directly detected by remote sensing, the variability in the relationship between the pigments and cyanotoxins – especially microcystins (MC), and the lack of standardization of the various measurement methods. A dual-model strategy can provide an approach to address these challenges. One model uses either chlorophyll-*a* (Chl-*a*) or phycocyanin (PC) collected *in situ* as a surrogate to estimate the MC concentration. The other uses a remote sensing algorithm to estimate the concentration of the surrogate pigment. Where blooms are mixtures of cyanobacteria and eukaryotic algae, PC should be the preferred surrogate to Chl-*a*. Where cyanobacteria dominate, Chl-*a* is a better surrogate than PC for remote sensing. Phycocyanin is less sensitive to detection by optical remote sensing, it is less frequently measured, PC laboratory methods are still not standardized, and PC has greater intracellular variability. Either pigment should not be presumed to have a fixed relationship with MC for any water body. The MC-pigment relationship can be valid over weeks, but have considerable intra- and inter-annual variability due to changes in the amount of MC produced relative to cyanobacterial biomass. To detect pigments by satellite, three classes of algorithms (analytic, semi-analytic, and derivative) have been used. Analytical and semi-analytical algorithms are more sensitive but less robust than derivatives because they depend on accurate atmospheric correction; as a result derivatives are more commonly used. Derivatives can estimate Chl-*a* concentration, and research suggests they can detect and possibly quantify PC. Derivative algorithms, however, need to be standardized in order to evaluate the reproducibility of parameterizations between lakes. A strategy for producing useful estimates of microcystins from cyanobacterial biomass is described, provided cyanotoxin variability is addressed.

Published by Elsevier B.V.

Contents

1. Introduction . . . 161
   1.1. Cyanotoxin issues, background and constraints . . . 161
2. Surrogate identification . . . 162
3. Modeling microcystin–pigment relationships . . . 162
   3.1. Microcystin–surrogate relationships . . . 162
   3.2. Comparing microcystins with surrogate pigments . . . 163
4. Modeling pigments from satellite . . . 165

* Corresponding author.
E-mail address: richard.stumpf@noaa.gov (R.P. Stumpf).

http://dx.doi.org/10.1016/j.hal.2016.01.005
1568-9883/Published by Elsevier B.V.

4.1. Analytical approaches . . . 165
4.2. Semi-analytical approaches . . . 165
4.3. Derivative approaches . . . 166
4.3.1. Derivative parameterization for PC . . . 166
4.3.2. Derivative parameterization for Chl-*a* . . . 166
4.3.3. Derivative sensitivity . . . 167
4.3.4. Derivative potential . . . 167
4.4. Cyanobacterial bloom climatology . . . 167
5. Applications . . . 168
5.1. Choice of surrogates . . . 168
5.2. Applications to mapping . . . 169
6. Analytical uncertainties . . . 169
7. Parameterization of the dual model . . . 170
8. Conclusions . . . 170
Acknowledgements . . . 171
References . . . 171

1. Introduction

Toxic cyanobacterial blooms are increasingly a public health and water management concern. These blooms occur globally, causing animal deaths, human health risks, expenses to public water suppliers and a nuisance to environmental and recreational management communities (Chorus and Bartram, 1999; Ibelings et al., 2014). The variety of cyanotoxins produced by cyanobacteria includes hepatotoxins (e.g. microcystins, cylindrospermopsin), and neurotoxins (e.g. anatoxins and saxitoxins). Microcystins (MC) are the most common, and are produced by the ubiquitous cyanobacterium, *Microcystis aeruginosa*, as well as several other cyanobacterial genera (O'Neil et al., 2012; Pearson et al., 2016). Identifying the presence and distribution of cyanotoxins in lakes and reservoirs will benefit water suppliers and public health managers.

Numerous studies have evaluated or applied remote sensing as a means of mapping, evaluating, or monitoring cyanobacterial blooms. These studies have proposed a variety of algorithms for detecting or quantifying cyanobacterial blooms with different sensors (see reviews by Kutser, 2009; Matthews, 2011; Sass et al., 2007). Satellites have been used for retrospective evaluation of cyanobacterial blooms (Binding et al., 2013; Kahru and Elmgren, 2014; Matthews et al., 2012; Moradi, 2014; Palmer et al., 2015b; Stumpf et al., 2012; Wynne et al., 2010), and as part of monitoring programs (Gómez et al., 2011; Wynne et al., 2013b; Zhang and Duan, 2008). Not all strains of *Microcystis* and other cyanotoxin-producing taxa produce cyanotoxins (O'Neil et al., 2012), therefore maps of bloom intensity cannot be assumed to translate to valid maps of cyanotoxin distribution.

Of the several cyanotoxins, MCs are the most understood and the most commonly monitored. Microcystins are not pigments and do not absorb visible or near-infrared (NIR) light (Al-Ammar et al., 2013), so remote sensing cannot directly detect them. Mapping MCs with remote sensing will then require a dual-model strategy: (1) characterizing a relationship between the cyanotoxin and a surrogate pigment that can be reliably detected by satellite and (2) establishing the relationship between satellite observations and the surrogate. This concept has been used in other remotely sensed applications for aquatic environments. One of the simplest examples involves estimating salinity in coastal waters using colored dissolved organic matter (CDOM) (D'sa et al., 2002; Salisbury et al., 2011). Satellite-derived optical properties are also used as input to more sophisticated models; for example, those for primary productivity use chlorophyll-*a* (Chl-*a*) and light attenuation estimates as inputs (Behrenfeld et al., 2006). A dual-model approach for MCs was presented by Shi et al. (2015) for Lake Taihu, China. They used a satellite model to estimate Chl-*a*, and then used a few weeks of field data to establish a fixed relationship between MC and Chl-*a*. They recognized that this relationship would be unlikely to apply to other lakes because of known variations in the relationship between MC and Chl-*a* (Ha et al., 2011; Shi et al., 2015); although they proposed that this relationship should apply routinely for Lake Taihu. Understanding the relationships between MCs and pigments will be necessary to the cyanotoxin modeling strategy.

The dual-model strategy is both necessary and advantageous to cyanotoxin mapping. From an analytical perspective, models that directly relate satellite observations to the MC concentration will over-fit the data, because the models typically have insufficient observations relative to the number of parameters, and because they inherently force a fit to the training set (Babyak, 2004). As a result, a single model is suitable only for the specific conditions for which it was developed. With the dual-model approach, parameterization, evaluation, and adjustment (or retuning) become simpler and more robust. Evaluating and retuning the cyanotoxin-surrogate model can be performed without any remotely sensed data, allowing updates through a season; similarly, the surrogate-satellite model can be evaluated and adjusted, if necessary, without the need for cyanotoxin data. Additionally, the uncertainties can be partitioned between models, such that sources of error or confusion can be identified.

Applying a dual-model strategy for cyanotoxins involves several challenges. These include the need for surrogate pigments, the variability in the relationship between cyanotoxins and pigments, and the lack of standardization of the various laboratory and remote sensing measurement methods. This paper will consider these issues in attempting to estimate MCs from satellite data by examining: (1) the issues involved with choosing surrogate pigment, (2) the characteristics of the MC-surrogate relationship, (3) the strengths and limitations of the classes of remote sensing models used for cyanobacterial blooms, and (4) the strategies and considerations for determining whether, and how, to implement the dual models in cyanotoxin mapping. For remote sensing, the emphasis will be on the medium resolution imaging spectrometer (MERIS) sensor and bands, as this sensor has proved the most useful for studies of cyanobacteria; and its replacement, the Ocean Colour Land Imager (OLCI) will be launched in early 2016.

1.1. Cyanotoxin issues, background and constraints

The World Health Organization (WHO, Chorus and Bartram, 1999) provided a widely used set of recommended action levels for risk associated with MC exposure (see also Chorus and Fastner, 2001; Falconer and Humpage, 2005). The WHO provisional guidelines use MC concentration of $>10\ \mu g\ L^{-1}$ in recreational

waters to indicate additional monitoring is needed to ensure public health protection; many states in the U.S. have developed guidance around the 10 μg L^{-1} threshold (Graham et al., 2009). When source-water supplies exceed the WHO finished-drinking water guideline of 1 μg L^{-1}, managers often initiate additional monitoring of source water or begin additional treatment of drinking water. Recognizing that chlorophyll is a biomass indicator and more frequently monitored than toxins, Chorus and Bartram (1999) also provided guidance using chlorophyll-*a*, suggesting that >10 μg L^{-1} of chlorophyll-*a* may indicate toxin concentrations that cause mild effects (e.g. contact dermatitis and gastrointestinal upset) during recreational contact. The essential assumption is that high biomass indicates a risk of high cyanotoxin concentration when cyanobacteria dominate the phytoplankton biomass. From a recreational perspective, health departments often provide warnings about avoiding discolored water and cyanobacterial scums (surface accumulations) through posted advisories, web-based sites, and social media (Chorus, 2005; Graham et al., 2009; Ohio EPA, 2015).

2. Surrogate identification

A surrogate has to be an indicator of cyanobacterial biomass and reliably quantifiable from satellite data. Chl-*a* is a common metric for algal biomass and is used as a reference for cyanobacterial blooms (Chorus and Bartram, 1999). Phycocyanins (PC) are recognized as indicators of cyanobacterial presence in eutrophic systems (De Marsac, 2003; Kirk, 1994), although they are also found in rhodophytes and some crytophytes (Wehr and Sheath, 2003). (Another phycobiliprotein, phycoerythrin, is a better indicator of cyanobacteria in more oligotrophic lakes and oceans, Kirk, 1994.) While many other metrics have been used with remote sensing to examine cyanobacteria, Chl-*a* and PC have been examined most closely (see reviews by Kutser, 2009; Matthews, 2011).

The decision on whether to use Chl-*a* or PC depends on three factors: availability, specificity, and sensitivity. Availability is the practical consideration of the availability of usable field and satellite measurements. Specificity involves the detection of cyanobacteria relative to eukaryotic algae when both are present. Sensitivity is the ability to detect meaningful differences in pigment concentration.

Availability favors Chl-*a*. Analysis of PC from water samples is uncommon relative to Chl-*a* analysis. The two pigments have to be treated separately – Chl-*a* is lipophilic while PC is hydrophilic – requiring different extraction solvents in the laboratory (Zimba, 2012). Chl-*a* is a standard water quality metric with well-established standard laboratory techniques (Trees et al., 1985). Phycocyanin is infrequently measured, does not have standard methods, and extracting the pigment from cells is challenging—some extraction methods leave more pigment in the cells than is removed (Lawrenz et al., 2011; Zimba, 2012).

The sensor spectral bands determine the availability of remote sensing methods to accurately distinguish and quantify the pigments. Phycocyanin absorbs most strongly around 620 nm (orange-red light), while Chl-*a* absorbs in the blue and red (maxima about 440 nm and 681 nm). This absorption reduces the reflectance at these wavelengths (Fig. 1), a factor in creating the characteristic green color of cyanobacterial blooms. Most sensors do not have a band specific to 620 nm so they cannot explicitly detect PC, whereas all existing sensors have bands that cover both the blue and red Chl-*a* absorption peaks. For those sensors without a band specific to PC, such as Landsat or Sentinel-2, Chl-*a* will inherently be the preferred indicator (Kutser, 2009; Matthews, 2011; Sass et al., 2007). In the case of the MERIS and OLCI, as well as hyperspectral instruments, a band is available at 620 nm, giving

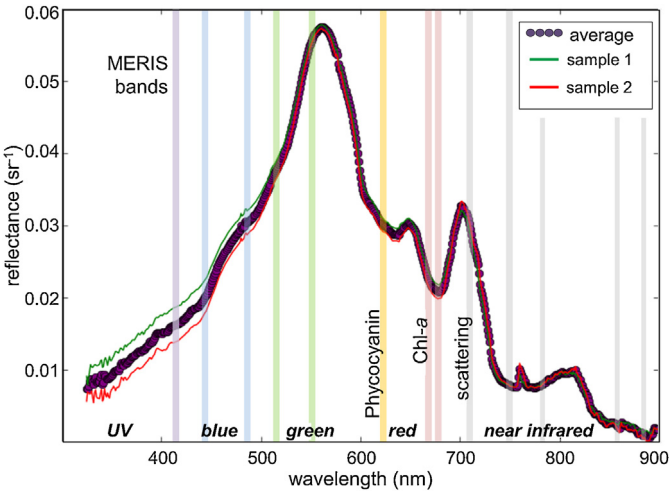

Fig. 1. Example remote sensing reflectance compared to wavelength obtained by handheld radiometer after Tomlinson et al. (2016). MERIS bands are denoted by vertical bars. Phycocyanin absorbs strongly about 620 nm, chlorophyll-*a* (Chl-*a*) between 665 to 681 nm, and water above 720 nm. The 709 nm band captures scattering from cells or sediment, between the absorption peaks of chlorophyll and water. Station average and replicates are shown.

the potential for detecting PC absorption. Other materials, such as sediment and CDOM absorb blue light, so bands around the Chl-*a* red absorption peak are needed for accurate discrimination of Chl-*a* from these other materials (Gitelson, 1992). MERIS and OLCI have multiple bands; Landsat has only one red band, reducing its utility for discriminating Chl-*a* from other pigments and sediments.

Specificity clearly favors PC, as it is an indicator pigment for cyanobacteria. In contrast, sensitivity favors Chl-*a*. At 620 nm, PC has a specific absorption of about 0.0075 m^2 mg^{-1}, while Chl-*a* at its absorption peak between 665 and 681 nm has a specific absorption of 0.015–0.02 m^2 mg^{-1} (Bricaud et al., 1995; Simis et al., 2005). This means that twice the concentration of PC to Chl-*a* is needed for the equivalent response in the satellite data. Also, Chl-*a*, and related chlorophylls (e.g. chlorophyll-*b* and chlorophyll-*c*) absorb at 620 nm, so PC concentration may be biased (over-estimated) in several remote sensing algorithms (Ruiz-Verdú et al., 2008; Simis et al., 2007). The presence and abundance of PC further varies with species composition, light spectral quality (more PC in water with strong attenuation of blue and green wavelengths), nutrient conditions, and physiological status of organisms (De Marsac, 2003; Reuter and Müller, 1993). While PC should be more specific to cyanobacteria, Chl-*a* may be more sensitive in detecting biomass variations in cyanobacteria-dominated blooms.

3. Modeling microcystin–pigment relationships

3.1. Microcystin–surrogate relationships

MCs are not always produced by cyanobacterial blooms, and even when produced, intracellular content may vary several orders of magnitude (Fastner et al., 2001; Ha et al., 2011) in response to various environmental factors. These cyanotoxins consist of a complex of amino acids, which require nitrogen. Consistent with this requirement, cellular production of MC appears to be greatest when nitrogen is abundant (Gobler et al., 2016; Monchamp et al., 2014; Orr and Jones, 1998). The amount of MC also varies with shifts in community composition of toxic and non-toxin strains, as non-toxic strains tend to grow faster under low light in the laboratory, suggesting they will grow faster in turbid water (Kardinaal et al., 2007; Briand et al., 2012). Non-toxic strains may

also dominate when inorganic nutrient concentrations are low (O'Neil et al., 2012). Given these factors, the specific concentration of MC to pigment (the ratio of concentrations) can be expected to vary. While there are large variations in MC occurrence (Davis et al., 2009, 2010; Graham et al., 2010), several studies have found constant ratios between MC and Chl-*a* over short periods of time (Ha et al., 2011; Lyck, 2004; Shi et al., 2015). The stability of these MC-pigment ratios for toxin estimation warrants closer inspection.

To examine this problem, a case study of the relationship between MCs and pigments uses data from three studies: one in Lake Erie, USA (Gobler et al., 2016), one on Long Island, New York (USA) (Davis et al., 2009), and a third from several U.S. Midwestern lakes (Graham et al., 2010). Particulate MCs, Chl-*a* and PC were measured for Lake Erie and Long Island as described in Davis et al. (2009, 2015a). Chl-*a* and total and dissolved MCs were measured in the Midwest study, with particulate MC calculated from the measured MCs; PC was not included in the Midwest study. Analytical methods used in these studies are not exactly the same. At the broad scales of comparison in this paper, however, differences between methods will not be substantive, but that should not be assumed to be the case when evaluating the narrower range of concentrations that may occur in a single water body. The Lake Erie and the Midwest MC data sets presented here came from Abraxis enzyme linked immune-sorbent assay (ELISA). Graham et al. (2010) also compared ELISA with LC/MS/MS and determined the various congeners and other toxins. For the Long Island lakes, Davis et al. (2009), used the protein phosphatase inhibition assay (PPIA, Carmichael and An, 1999). Carmichael and An (1999) compared PPIA with ELISA; the two methods produce similar results but the paper should be consulted for details. In addition, the Midwest lakes were examined for relative cyanobacterial abundance. Only samples where cyanobacteria constituted more than 90% of the phytoplankton biovolume are considered here and all but one were >95%. The Lake Erie data set came from a weekly monitoring program of fixed stations, allowing a rare evaluation of temporal variability in the relationships. The Long Island and Midwest data sets came from more opportunistic sampling. Microscopy was used only for qualitative inspection of the Lake Erie and Long Island data.

3.2. Comparing microcystins with surrogate pigments

The Lake Erie monitoring program provided a comprehensive data set of MC and pigments for 2013 and 2014. In 2013, the bloom started the last week of July; in 2014 it began several weeks earlier. In both years, MC broadly correlated with Chl-*a* and PC over the season, with similar relationships for the two years (Fig. 2, Table 1). While good relationships exist over the range of measurements, the logarithmic plots needed to show the three orders of magnitude range obscure the order of magnitude (10-fold) variations in MC concentration relative to pigment concentration (Fig. 2). As the uncertainty is proportional to the concentration, use of regression requires a log-transform of the data in order to establish appropriate relationships between MCs and pigments (Table 1). The residual standard error (RSE; nominally a standard deviation from the predictor line) is 2.7-fold in 2013 and 3.7-fold in 2014, leading to standard uncertainty ranges of 7- to 14-fold for models based on the full season of data. Such a large uncertainty is consistent with previous studies where the ratio of MC to Chl-*a* typically varied at least one order of magnitude over the season (Ha et al., 2011; Kardinaal et al., 2007; Kardinaal and Visser, 2005), indicating that single fixed relationships are unlikely or uninformative.

While the spread of the MC data around the relationship line might be presumed to be random variability, the pigment specific concentration (biomass or pigment normalized) of MCs indicates

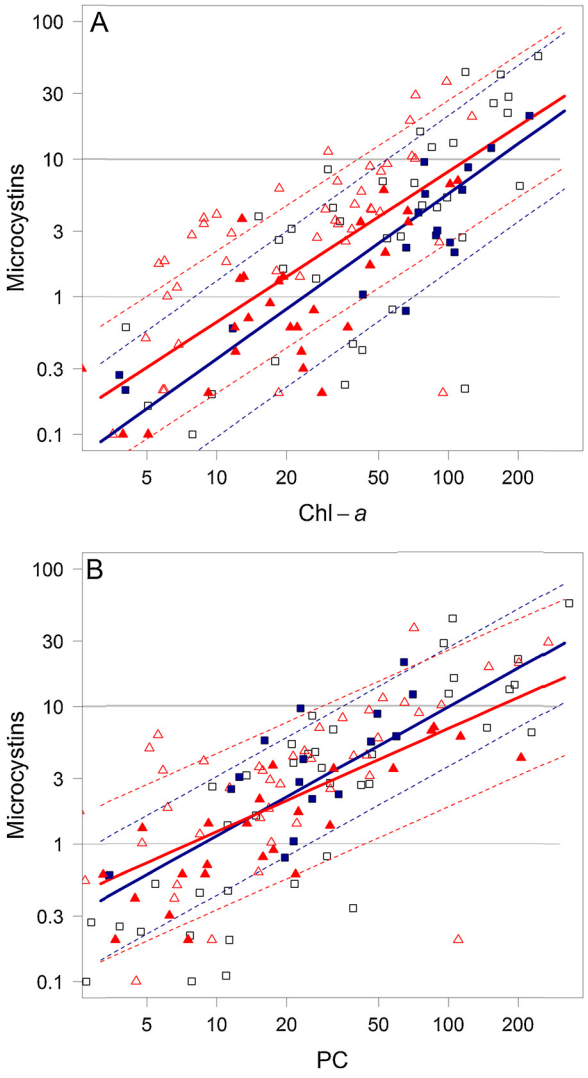

Fig. 2. Data and relationships for microcystins against *in situ* (a) chlorophyll-*a* (Chl-*a*) and (b) phycocyanin (PC), all collected from Lake Erie. Black and squares are from 2013; and red and triangles are from 2014. Filled values are observations from September. Solid lines are the relationships for all data for each year; dotted lines are the RSEs for the two relationships from Table 1. All units are $\mu g\ L^{-1}$. For PC, R^2 = 0.7 in 2013, and = 0.44 2014. For Chl-*a*, R^2 = 0.70 in 2013, and = 0.57 in 2014.

that the spread is caused by temporal variability in the presence of MC (Fig. 3). In 2014, the specific concentration of MC (MC/pigment) decreased substantially from July to September for both PC (median MC/PC decreasing from 0.20 to 0.08) and Chl-*a* (median MC/Chl-*a* decreasing from 0.19 to 0.06), a trend similar to that reported by Kardinaal et al. (2007) in Netherland lakes. In 2013, MC/PC fluctuated without a trend after July 25, but MC/Chl-*a* decreased from early August (median 0.15) to September (median 0.04). These variations indicate that the relationships cannot be assumed to be fixed throughout the season and also that the two pigments can have different behaviors relative to MC.

Examining shorter time periods reveals additional characteristics of the relationship between MC and the pigment. The uncertainty around the calibration lines decreased for shorter time periods. The early period (late July and early August) had an RSE of about 1.6-fold in both years, which produces an uncertainty range of 2.56 compared to the ~10-fold range for the tuning of the entire season. In September, the uncertainties increased but were still less than those for the full data set. The relationships between MC

Table 1
Example variation in parameterization for MC against PC and Chl-*a* tuned for western Lake Erie from different time periods in 2013 and 2014. A_0 and A_1 are parameters from log-transformed linear regression, where $\log MC = \log A_0 + A_1 \times \log$ (pigment), which transforms to the power law: $MC = A_0 \times (\text{pigment})^{A_1}$. R^2 is the squared regression coefficient, RSE is the residual standard error, which is a multiplier. A_1 and RSE units are dimensionless (dl). The PC and Chl-*a* concentrations are those that will give MC of 1.0 or 10 μg L^{-1} in each parameterization. If $A_1 = 1$, the relationship is linear, and A_0 is the slope, i.e., $MC = A_0 \times$ (pigment). Regression-based uncertainties for A_0 and A_1 fall within narrow ranges: multiplier of 1.3–1.5 for A_0 and ± 0.08 to 0.14 for A_1.

PC	A_0 (μg L^{-1})	A_1 (dl)	R^2	RSE × (dl)	PC (μg L^{-1}) for MC = 1.0	PC (μg L^{-1}) for MC = 10
2013 all (29 Jul–22 Sep)	0.13	0.94	0.70	2.7	8.8	103
2014 all (21 Jul–06 Oct)	0.22	0.75	0.44	3.7	7.5	162
2013 29 Jul–12 Aug	0.38	0.73	0.81	1.6	3.7	87
2013 19 Aug–31 Aug	0.07	1.33	0.67	3.0	14	438
2013 03–22 Sep	0.44	0.61	0.65	2.0	3.4	109
2014 29 Jul–04 Aug	0.52	0.67	0.77	1.5	2.7	84
2014 11 Aug–31 Aug	0.06	1.12	0.63	2.8	12	94
2014 02–29 Sep	0.17	0.70	0.67	3.4	12	310
Chl-*a*	A_0 (μg L^{-1})	A_1 (dL)	R^2	RSE × (dL)	Chl-*a* (μg L^{-1}) for MC = 1.0	Chl-*a* (μg L^{-1}) for MC = 10
2013 all (29 Jul–22 Sep)	0.022	0.93	0.70	3.7	24	161
2014 all (21 Jul–06 Oct)	0.052	1.20	0.57	3.3	15	120
2013 29 Jul–12 Aug	0.10	1.09	0.84	1.5	8.3	69
2013 19 Aug–31 Aug	0.0017	1.80	0.83	2.2	33	120
2013 03–22 Sep	0.076	0.88	0.76	1.9	19	252
2014 29 Jul–04 Aug	0.30	0.82	0.83	1.4	4.5	75
2014 11 Aug–31 Aug	0.002	1.78	0.81	2.1	30	109
2014 02–29 Sep	0.042	1.01	0.57	2.2	23	225

and pigments also changed over time. The pigment concentrations needed to predict threshold MCs increased over the season—consistent with Kardinaal et al.'s (2007) observations. While MC and the pigments had similar relationships in early August in both years (e.g., MC of 10 μg L^{-1} corresponds to about 80 μg L^{-1} of PC and 70 μg L^{-1} Chl-*a*, Table 1), the relationships differed greatly between the two Septembers. There was 3-fold more MC relative to PC in September 2013 than 2014 (filled symbols in Fig. 2B, and Table 1), while 2013 and 2014 had similar patterns of MC against Chl-*a* (Fig. 2A). The data sets provided other evidence that

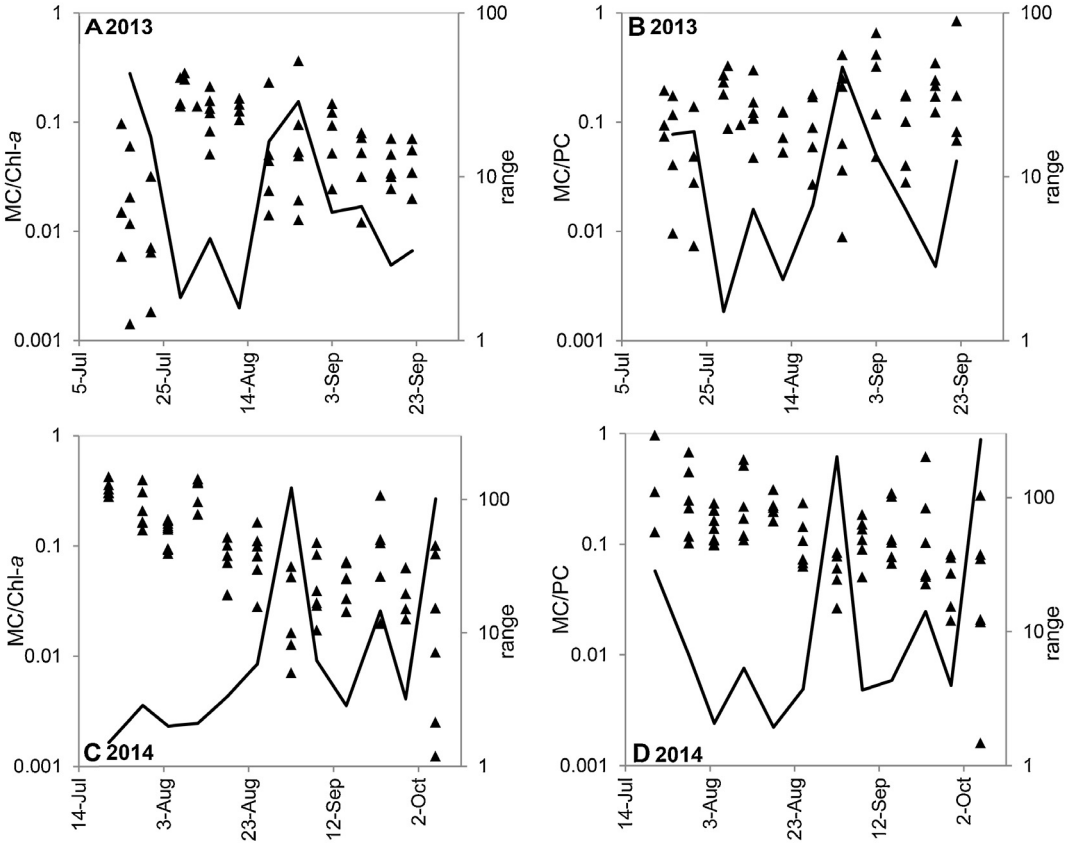

Fig. 3. Time series of the specific concentration of microcystin (MC) relative to chlorophyll-*a* (Chl-*a*) or phycocyanin (PC) from the Lake Erie data (triangles) and the range on each date (line), which is the ratio of the highest to lowest specific concentration. Lower range means less variation in the specific concentration, a range value of 1 would occur if all samples on the same day had the same MC/pigment ratio. All constituents had units of μg L^{-1}, the ratios are all dimensionless. Six fixed stations within a 500 km^2 area of southwestern Lake Erie were sampled on a single day each week.

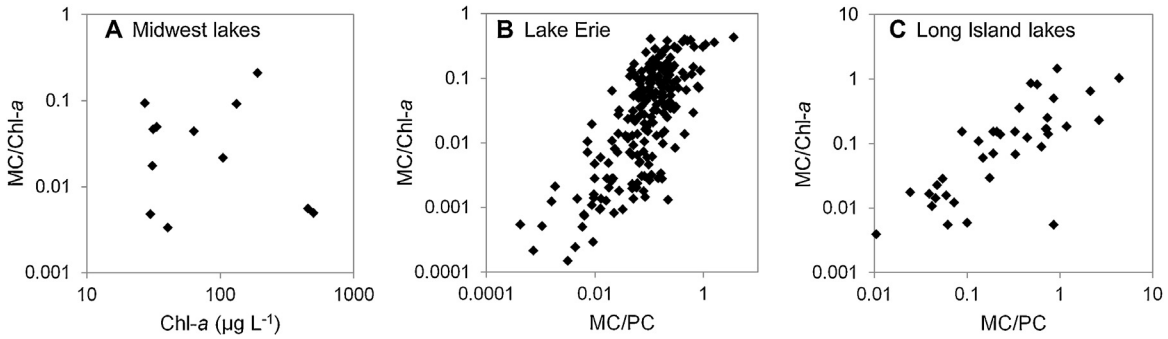

Fig. 4. Pigment-specific concentrations of microcystins (MC). Phycocyanin (PC) is not available for the Midwest lakes. Data from Davis et al. (2009) and Graham et al. (2010).

parameterizations should not apply across years. At low pigment concentrations (PC < 10 μg L^{-1} and Chl-*a* < 14 μg L^{-1}), MC concentration were consistently below 1 μg L^{-1} in 2013, but reached 7 μg L^{-1} in 2014.

The Long Island and Midwest lakes showed similar ranges of pigment-specific concentrations to Lake Erie (Fig. 4) with MC/Chl-*a* and MC/PC varying the same several orders of magnitude. The MC/Chl-*a* for the Midwest lakes ranged two orders of magnitude in the mid-range of the other two studies, even though the samples included mixed cyanobacterial assemblages that varied from virtually no *Microcystis* to all *Microcystis*. The variability seen in the other lakes results from spatial differences between lakes (Midwest, Graham et al., 2009) as well as temporal variability within lakes (Long Island, Davis et al., 2009). The Lake Erie data set shows, however, that usable relationships with reasonable uncertainties can be established by constraining the time scales to weeks. Capturing the temporal variability in order to establish and maintain accurate models between MC and the pigments will require routine monitoring programs in the lakes of interest.

4. Modeling pigments from satellite

The second part of the dual model involves estimating the pigments from remotely sensed data. There are several classes of algorithms that can be used to estimate cyanobacterial abundance or biomass from Chl-*a* or PC. These classes can be described as follows: analytical, semi-analytical, and second derivative (or spectral shape). Analytical approaches (also called inversion algorithms) solve simplified forms of the radiative transfer equation to extract the spectral absorption of the various constituents (phytoplankton, CDOM, sediment) from the calculated water reflectance. Laboratory measurements of pigment-specific absorption are used to equate these to Chl-*a* and PC. Semi-analytical algorithms (sometimes called empirical algorithms) use bio-optical principles, frequently applied with ratios, to extract relative pigment concentrations from the calculated water reflectance. They are parameterized empirically, typically using regression of field measurements with either field radiometry (simulating the satellite) or satellite data. The derivative algorithms can be described as the distance of an intermediate point from a baseline of adjacent points (Letelier and Abbott, 1996; Philpot, 1991), with the band selection based on optical properties, and the parameterization using a regression-type solution, like the semi-analytical algorithms. They do not require an atmospheric correction to solve for water reflectance and, so, can be applied to the reflectance measured at the satellite.

4.1. Analytical approaches

Analytical approaches involve solving for backscatter and absorption from water reflectance in multiple bands and parsing these into absorption by Chl-*a* and PC (Simis et al., 2005; Mishra et al., 2013). Most are based on Simis et al. (2005) and have been reviewed in some detail elsewhere (Matthews, 2011; Ruiz-Verdú et al., 2008). These have been shown to be quite effective with field data collected by radiometry. They are also effective in explicitly solving for pigments separately from sediment or CDOM. The challenge in applying analytical approaches to satellite data is the need for accurate water reflectance as an input, which requires an accurate atmospheric correction. Atmospheric correction in turbid water is a difficult task, particularly with blooms that can directly alter the NIR reflectance used in the correction. If glint (direct reflection of sunlight off the water to the sensor) is present, the atmospheric correction becomes even more challenging. In extreme cases of error, one or more spectral bands are over-corrected to the point of having "negative" reflectance, a physical impossibility that leads to algorithm failure. Wynne et al. (2010) estimated that 25% of atmospherically-corrected MERIS data from western Lake Erie had negative reflectance during the bloom season. The atmospheric correction could be performed on individual scenes, but this is tedious and would reduce the effectiveness of a satellite monitoring program. Furthermore, while negative reflectance values indicate the most extreme error in atmospheric correction, positive reflectances can also be in error—errors that propagate into the models (Wang and Shi, 2007). The need for accurate atmospheric correction over an entire water body reduces the robustness of these methods, limiting the usable data they can provide.

4.2. Semi-analytical approaches

The most common semi-analytical approaches involve ratio algorithms, which are based on empirical solutions to simplified versions of the radiative transfer equation (Gordon and Morel, 1983). While water strongly absorbs NIR light, dense algal blooms produce enough water reflectance in the NIR – particularly in bands between 700 nm and 750 nm – to be effective in ratio algorithms for Chl-*a* (Gilerson et al., 2010; Gitelson, 1992; Moses et al., 2012; Stumpf and Tyler, 1988). These approaches have also been used for PC (Gómez et al., 2011; Mishra et al., 2009, 2013; see also review by Matthews, 2011). Ratio type algorithms also implicitly correct for sediment backscatter (Gordon and Morel, 1983). While still requiring an accurate atmospheric correction, these methods are more robust than analytical solutions in that the calculation is a ratio, rather than a system of equations. A ratio can partially offset some residual error in atmospheric correction (Stumpf and Tyler, 1988). Failure still occurs with negative reflectances, and large biases will occur when the input water reflectance is severely underestimated (Wang and Shi, 2007).

Ratio algorithms have particular value to sensors with few bands such as Landsat, with ratios of blue to green or blue to red

bands providing useful information on Chl-*a* concentration in specific lakes (reviews by Sass et al., 2007; Matthews, 2011). The Chl-*a* relationships are highly dependent on comparatively negligible absorption by other blue absorbing pigments, such as CDOM, so they are unlikely to work consistently across lakes with differing optical properties (Matthews, 2011). Landsat data sets are typically processed manually (Olmanson et al., 2011), and systematic automated methods have not yet been demonstrated.

Ratios parameterized for MERIS have shown promise for systematic regional applications. Gómez et al. (2011) observed consistent results across several lakes in Spain using a fixed parameterization for PC. Gilerson et al. (2010) found a consistent parameterization applied to both Chesapeake Bay and Nebraska lakes (based on field radiometry). While the ratio algorithms are useful, the problem of accurate atmospheric and glint correction still constrains the frequency of data they can provide for routine monitoring from satellite.

4.3. Derivative approaches

Derivative algorithms are also called spectral shape, curvature, or baseline algorithms. These include the maximum chlorophyll index (MCI; Gower et al., 2005), the cyanobacterial-related chlorophyll index (CI; Wynne et al., 2008), the floating algae index (FAI; Hu, 2009), and the maximum chlorophyll height (MPH; Matthews et al., 2012). These algorithms quantify the curvature of "peaks" or "valleys" in the reflectance spectra that result from sharp changes in the absorption spectra. The MCI, CI, and MPH estimate Chl-*a* concentration using the "red edge" (between 665 nm and 754 nm) caused by the differential absorption by Chl-*a*. Chl-*a* absorbs strongly at 665 and more so at 681 nm, whereas water absorbs strongly at 754 nm, while neither material absorbs as strongly around 709 nm (Fig. 1). The FAI measures the strong reflectance of the NIR (860 nm), caused by scattering from cells lying on the water surface, relative to the weak reflectance of the red and short-wave infrared (found on MODIS or Landsat), caused by absorption of those wavelengths by the cells. Unlike the other metrics, the FAI estimates only scum coverage and density (Hu et al., 2010) and not Chl-*a* concentration. MERIS does not have SWIR bands, but the other derivatives designed for MERIS (MCI, CI, and MPH) can detect both chlorophyll concentration and scum density (Matthews et al., 2012; Wynne et al., 2013a,b).

These algorithms are all take the form of second derivatives (Philpot, 1991; Stumpf and Werdell, 2010), namely:

$$SS(\lambda) = R(\lambda) - R(\lambda_-) + (R(\lambda_-) - R(\lambda_+)\frac{(\lambda - \lambda_-)}{(\lambda_+ - \lambda_-)}$$

where R is the reflectance (or radiance), λ is the central band, and λ_+ and λ_- are the adjacent reference bands. Philpot (1991) showed that second derivatives implicitly remove most of the atmospheric signal, making them more robust than the analytical and ratio methods. As a result, when applied to satellite, derivatives typically use top of atmosphere (TOA) data. Gower et al. (2005) applied this capability by developing the original MCI with TOA radiance, meaning no atmospheric correction at all. Long spectral baselines (e.g. 200 nm or more), may begin to have errors if fine-mode aerosols appear, as these aerosols introduce a trend in the reflectance spectra. The methods can be applied under conditions of mild sun-glint, because glint is spectrally flat (Hu et al., 2012). As a result of the much greater frequency of coverage compared to the analytical and ratio methods, these algorithms have become the most common method used for bloom analyses and routine monitoring (Matthews et al., 2011; Wynne et al., 2013b) and for phenological and climatological studies of lakes (Binding et al., 2011; Duan et al., 2014; Matthews, 2014; Moradi, 2014; Palmer et al., 2015b; Stumpf et al., 2012).

Derivatives tend to be re-parameterized in each lake, rather than evaluating the reproducibility of an existing parameterization such as was done by Lunetta et al. (2015), or is typically done with the analytical and ratio algorithms. One problem is that both TOA radiance (Binding et al., 2012; Gower et al., 2005; Palmer et al., 2015a) and TOA reflectance (Binding et al., 2012; Stumpf et al., 2012; Wynne et al., 2013a; Matthews, 2014) have been used. Because the derivative uses differences, the variation in sunlight with latitude and season will alter the magnitude of the result if radiance is used, and the resulting products cannot be converted to reflectance (which is corrected for sun elevation). As a result, radiance products cannot be validly compared across different latitudes or seasons. This is a consideration for any algorithm that involves sums; radiance and reflectance are not interchangeable, and reflectance should be used for reproducibility.

4.3.1. Derivative parameterization for PC

Compared to Chl-*a*, PC has had limited study with second derivatives. In Lake Taihu, China, which typically has intense scum-forming cyanobacterial blooms, Qi et al. (2014) developed a model that uses the shape at 550, 620, and 665 nm to correlate with high concentrations of PC. Water also has a strong differential absorption between 550 nm and 620 nm. This means that in water with high concentrations of scattering particles, the curvature caused by water absorption will be confused with that caused by PC absorption, an issue not examined in their study. Matthews et al. (2012) and Lunetta et al. (2015) used a derivative with the 620, 665, and 681 nm bands on MERIS to indicate presence or absence of cyanobacteria, based on the PC absorption. The rationale follows that used in analytical methods (Simis et al., 2005; Mishra et al., 2009), namely that PC at 620 nm and Chl-*a* at 681 nm lower the reflectance at these wavelengths relative to 665 nm, resulting in a positive SS(665) (creating an upward bump between 620 nm and 681 nm in Fig. 1).

Currently, no direct comparison of the SS(665) with PC has been made, partly from the lack of PC laboratory measurements. Cell counts of *Microcystis* can provide a surrogate for PC in order to assess the potential of the derivative for estimating relative amounts of PC. Field reflectance measurements from the Chesapeake Bay area during *Microcystis* blooms show that SS(665) co-varies with cell counts as predicted by the influence of PC (Fig. 5). Positive SS(665), the condition used to identify the presence of cyanobacteria (Lunetta et al., 2015; Matthews and Odermatt, 2015) did not occur until cell counts exceeded 10^4 cells mL^{-1}. This threshold is reasonable, particularly as that cell concentration may correspond to about 5 $\mu g\ L^{-1}$ Chl-*a* (Chorus and Bartram, 1999), which is below the sensitivity (Section 4.3.3) of the derivative methods for Chl-*a*. The SS(665) will need additional comparison with laboratory PC measurements for validation and parameterization.

4.3.2. Derivative parameterization for Chl-a

While derivative algorithms are relatively insensitive to atmospheric errors, they have some limitations. The MCI is sensitive to suspended sediment at moderately low Chl-*a* concentrations (Binding et al., 2012). Gordon and Morel (1983) showed that difference algorithms can confound Chl-*a* and sediment when applied to reflectance peaks (which the MCI specifically captures). The CI includes the differential absorption by Chl-*a* between 665 and 681 nm (greater Chl-*a* absorption at 681 nm than at 665 nm), so the algorithm should be less sensitive to suspended sediment than the MCI.

Because Chl-*a* fluoresces at about 681 nm, the fluorescence peak essentially overlays the Chl-*a* red absorption maximum. As a result, the CI has the interesting property of using the same satellite band set as that used to estimate fluorescence in

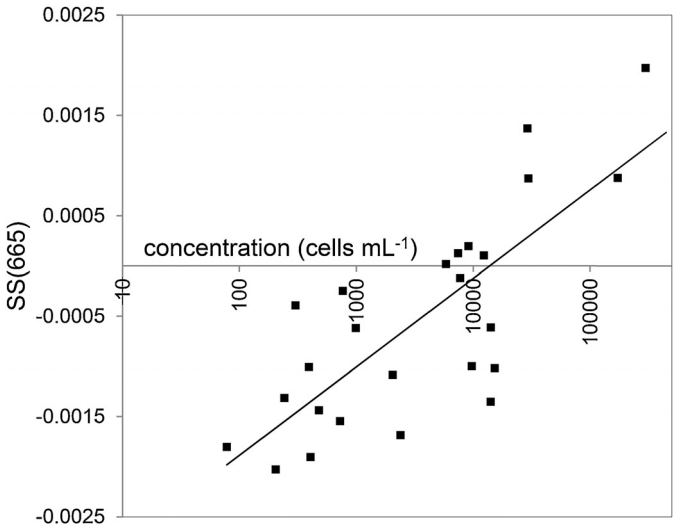

Fig. 5. Derivative centered on MERIS 665 nm band against cell count per mL^{-1} of *Microcystis* spp. R^2 = 0.60. Horizontal axis is set at SS(665) = 0, the threshold used to identify cyanobacterial blooms (see text). The MERIS was simulated using methods of Tomlinson et al. (2016) and compared to microscopic cell counts by the Maryland Department of Natural Resources.

eukaryotic algae with a product called fluorescence line height (FLH). This has been a confusing result (Binding et al., 2011; Matthews and Odermatt, 2015; Palmer et al., 2015a,b); positive SS(681), i.e., FLH, indicates fluorescence consistent with the presence of eukaryotic algae and negative SS(681), i.e., CI, indicates Chl-*a* absorption (in the absence of fluorescence) that is more consistent with the amount of cyanobacteria. The reason is straightforward. In cyanobacteria, Chl-*a* is deployed mostly in Photosystem I, where it does not fluoresce, while eukaryotes deploy most Chl-*a* in Photosystem II, which leads to fluorescence. As a result, cyanobacteria produce less than 20% of the Chl-*a* fluorescence of eukaryotes (Seppälä et al., 2007). For cyanobacteria, the weak fluorescence means that the increased Chl-*a* absorption dominates the reflectance spectrum around 681 nm. Chl-*a* absorbs more strongly at 681 nm than at 665 nm, so less light leaves the water at 681 nm causing a "dip" in reflectance (Fig. 1). For eukaryotes, light emitted by Chl-*a* fluorescence, when combined with the reflected light causes more light to leave the water at 681 nm than at 665, producing the fluorescence peak (FLH, Letelier and Abbott, 1996) in reflectance spectra observed for these algae. This result means the calibration of SS(681) to Chl-*a* must distinguish cyanobacteria from eukaryotes, as the same Chl-*a* concentration can produce negative SS(681) in cyanobacteria blooms and positive SS(681) in eukaryotic algal blooms. The confusing term "negative FLH" has been used in the literature for the drop in reflectance at 681 nm; this term should be discouraged as it is scientifically invalid – fluorescence cannot be negative – and the phenomenon is caused by Chl-*a* absorption. The "CI" is the appropriate term for the metric derived from negative SS(681) (Wynne et al., 2008).

4.3.3. Derivative sensitivity

The range of concentrations detected by derivatives differs from the analytical and ratio methods. Unlike the latter methods, the derivatives used for cyanobacteria can provide quantitative data in dense scums, so there is no obvious upper limit on pigment concentrations (except analytical uncertainty). At lower concentrations, derivatives are less sensitive. The analytical methods can detect pigments to 1–5 $\mu g\ L^{-1}$ and lower with algorithm switching (Gilerson et al., 2010; Gons et al., 2008). The MCI has a minimum threshold of $<10\ \mu g\ L^{-1}$ of Chl-*a* (Palmer et al., 2015a). While the MPH can detect lower Chl-*a* concentrations in eukaryotic blooms by switching to fluorescence detection, it uses the same 709 nm band as does the MCI for cyanobacteria (Matthews and Odermatt, 2015), so it should have the same Chl-*a* limit as the MCI for these blooms. The lower threshold for the CI is not known; however observations on Lake Erie show that the CI does not pick up concentrations as low as the MCI. Tomlinson et al. (2016) found that in some Florida lakes the CI threshold falls below 16-20 $\mu g\ L^{-1}$, although plots in Palmer et al. (2015b) suggest that 10 $\mu g\ L^{-1}$ is possible. This threshold may be a function of the background concentration of eukaryotic algae.

These thresholds of detection are appropriate for assessing toxicity risk. Toxic cyanobacterial blooms occur in eutrophic waters (Downing et al., 2001). Carlson (1977) gave a Chl-*a* threshold for eutrophic lakes of 20 $\mu g\ L^{-1}$, and Chorus and Bartram (1999) put 10 $\mu g\ L^{-1}$ as a threshold between negligible and moderate risk. Equivalent thresholds for PC do not exist owing to the paucity of data. Because the FAI detects only surface accumulations, and determining Chl-*a* concentration in scums is problematic, it should be treated as a simple metric of the amount of scum in each pixel. This is analogous to how the normalized vegetation index for land is used to infer the relative density of live biomass in each pixel (Becker and Choudhury, 1988). In terms of *Microcystis* cells, the CI likely has a threshold between $1 \times 10^4$and 2.5×10^4 cells mL^{-1} (Wynne and Stumpf, 2015). This is below the WHO risk level for cell concentration; however, conversions to cells or biovolumes have not been made for other species or algorithms. Relationships between Chl-*a*, PC, and biovolume continue to be explored (Kasinak et al., 2015).

4.3.4. Derivative potential

Most derivatives have been tuned with matchups between water samples and satellites. By comparison, the analytical and ratio methods have been tuned by simulating the satellite reflectance with radiometric measurements in the field of the water being sampled. This field radiometry allows collection of more observations and eliminates the misfit introduced because of the considerable differences in scale between water samples and satellite pixels (Kutser, 2009). Field radiometry can be effective for tuning derivatives (Tomlinson et al., 2016), providing data of better quality for quantification of the algorithms than comparisons of satellite and field data.

Of the three classes of methods, the analytical and semi-analytical will be appropriate for non-satellite platforms or when observation frequency is not a concern in the satellite data. When frequency of coverage is needed, however, derivatives are superior. Derivative metrics can also be applied seamlessly from water column concentrations to scum concentrations (Matthews and Odermatt, 2015; Wynne et al., 2013a), which is not possible with analytical methods. Work is still needed on directly quantifying PC from derivatives, but this may prove to be a solvable problem (Section 4.3.1).

4.4. Cyanobacterial bloom climatology

Caution should be used in the application of all the satellite methods for development of climatologies of cyanobacterial bloom characteristics. Between the turbidity of the water in these blooms and the strong absorption of light by water at red wavelengths, only surface concentrations can be determined. In a thin bloom, light is detected from the upper meter of water; whereas in scums, no information is retrieved from below the surface. For scum-forming cyanobacteria, such as *Microcystis*, the maximum buoyancy occurs with low irradiance, and cells typically float upward through the night or in turbid water (Visser et al., 2005). Calm winds will allow the biomass to accumulate at or near the surface; moderate

and strong winds will mix the biomass vertically, diluting and substantially reducing the surface concentration seen with satellite (Hunter et al., 2008; Hu et al., 2010; Wynne et al., 2010). Seasonal or inter-annual variations in wind may produce severe biases in estimating the seasonal bloom quantity. In the extreme case, the FAI, as a scum metric, will provide no information on the bloom when the wind has mixed the scum into the water column. (Hu et al., 2010) found that changes in wind speed from only 2 m s^{-1} to 3 m s^{-1} over consecutive days decreased the FAI bloom area from >1000 km^2 to <100 km^2. They recommended using only the maximum area observed in each month in building a bloom climatology for quantitative analysis. Other studies have compensated for the wind bias with other metrics. Kahru and Elmgren (2014) used maximum extent and duration in the Baltic. Palmer et al. (2015b) used phenological metrics, such as first and last day of detection, which depend much less on absolute concentrations. Stumpf et al. (2012) used 10-day composites of the maximum CI concentration to estimate the areal biomass in Lake Erie. Weather systems tend to pass through that region every 5–7 days and the cells would accumulate near the surface during the calm weather period (Wynne et al., 2010), providing a more consistent measure of the amount of biomass. If temporally-averaged concentrations are used, the wind impact on the surface concentration must be modeled and addressed. Wynne et al. (2010) showed that a simple model of mixing can provide estimates of total biomass to compensate for variation in surface concentration. Using these approaches will lead to the development of a robust climatology of the bloom characteristics.

Because MC presence varies through the season, establishing a climatology of MC distributions will be problematic without past data on the MC-pigment relationships at weekly or biweekly resolution. Otherwise, the large uncertainties in MC concentration estimates will produce unacceptable errors in any retrospective analysis. Studies of past conditions should concentrate on the bloom characteristics, rather than inferring the amount of toxicity.

5. Applications

5.1. Choice of surrogates

The choice of Chl-*a* or PC as the surrogate depends on several factors, particularly the trade-off between sensitivity and specificity. The balance lies with sensitivity for Chl-*a* against specificity for PC. For a lake with a spatially-variable mixed bloom of cyanobacteria and eukaryotic algae, PC should be the best surrogate (assuming there are limited cryptophytes or rhodophytes) as Chl-*a* is non-specific for cyanobacteria. For blooms with biomass dominated by cyanobacteria, Chl-*a* offers sensitivity for remote sensing that presents an advantage over PC.

As described in Section 2, Chl-*a* absorbs 2–3 times as much light at 665–681 nm as PC absorbs at 620 nm. This means that the PC concentration must be about two times that of Chl-*a* for the same remote sensing detection sensitivity. This proportion is not a common phenomenon in these lakes (Fig. 6); in fact the median PC/Chl-*a* ratio during cyanobacterial blooms was about 0.5 in Lake Erie, 0.3 in Long Island, and less than 1 in most cases (e.g. Fig. 6). Similar ratios occur in other water bodies, such as lakes in the Netherlands (Simis et al., 2007) and ponds in the southern US (Kasinak et al., 2015), although Spanish lakes have PC/Chl-*a* ratios >1 (Simis et al., 2007). For a median PC/Chl-*a* ratio of 0.5, the combination is a four-fold difference in sensitivity. Under this example, if the minimum algorithm detection is 10 μg L^{-1} of pigment, satellite will not detect a bloom with PC until the bloom Chl-*a* concentration exceeds 40 μg L^{-1}.

Even with PC algorithms there are additional issues to consider. Phycocyanin is not as stable an indicator of biomass as Chl-*a* within cyanobacterial blooms, as PC varies with light and nitrogen availability (Chaffin et al., 2012; Kirk, 1994). Both PC and MC may co-vary with nitrogen availability, an advantage for PC as a surrogate (Briand et al., 2012; Gobler et al., 2016; Monchamp et al., 2014; Oliver et al., 2012; Raven, 1984). Cellular PC content tends to increase with reduced (blue and green) light, however, while non-toxic *Microcystis* strains may out-compete toxic strains in low light (Briand et al., 2012; Kardinaal et al., 2007). The result is that light availability may push PC and MC concentrations in opposite directions, a disadvantage for PC as a surrogate. The Lake Erie measurements (Fig. 3) of MC specific concentration give credence to these problems. Relative to Chl-*a*, MC has somewhat more scatter over the entire season in the two years (Fig. 2 and RSE in Table 1), but on over half of the sample days in both years the MC/Chl-*a* ratio had a smaller range than MC/PC (Fig. 3). This is especially obvious early in 2014 (Fig. 3D). The range in MC/PC (measured as ratio of the highest to lowest values observed on the day) varied from 28- to 7-fold, while MC/Chl-*a* varied only 1.5 to 3-fold. During the rest of the time MC/Chl-*a* range was smaller than MC/PC over half of the days. The significant exception occurred in July 2013. The MC/Chl-*a* ratio was larger during a time when the bloom appeared to be mixed with diatoms; curiously though, this time also had a large range of MC/PC relative to later in the season. The range of variation in MC/pigment of the Long Island lakes was also the same for both pigments indicating no advantage for PC in those lakes (Fig. 4B).

From a practical point of view, the three derivative algorithms, CI, MCI, and MPH, all target Chl-*a*, so Chl-*a* is clearly the available surrogate for these algorithms. These methods have been demonstrated to accurately estimate Chl-*a* biomass in cyanobacterial blooms in specific areas. They have not been evaluated for the robustness of their parameterizations across different regions.

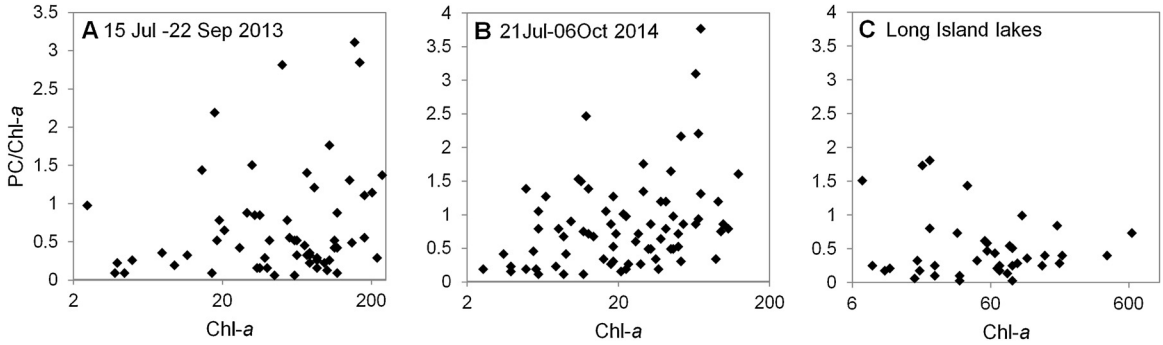

Fig. 6. Ratio of PC to Chl-*a* (dimensionless) against Chl-*a* concentration (μg L^{-1}) for Lake Erie, 2013, 2014, and Long Island lakes (Davis et al., 2009). The median PC/Chl-*a* for the three data sets are 0.51 (2013), 0.62 (2014), and 0.31 (Long Island).

Derivative algorithms for PC are quite new. The SS(665) has been used as an indicator (Lunetta et al., 2015; Matthews and Odermatt, 2015) and correlates with the concentration of *Microcystis* (Fig. 5), but it has not yet been related to PC concentration. The relative paucity of PC data for parameterization or validation remains a problem for all methods. As discussed in Section 2 (and below in Section 6), PC measurement is not standardized, so consistency or reproducibility may suffer as well. In short, while PC is a better surrogate for known mixed blooms, Chl-*a* has a practical advantage for use as a surrogate in cyanobacterial-dominated blooms.

5.2. Applications to mapping

The potential value of estimating MCs with a dual-model strategy can be seen in Fig. 7. Scenes of Lake Erie in early August and late September 2014 were processed to Chl-*a* from CI per methods of Wynne et al. (2013a) and Tomlinson et al. (2016), and MC was estimated using the Chl-*a* parameterizations for early August and late September (Table 1). The Chl-*a* concentrations were higher in September, but the MC concentrations were much lower (Fig. 7), the result of the much lower specific concentration in September (Fig. 3C). As a result, the water in September contained as much biomass (and discoloration) as in early August, but the health risk from the toxin was potentially much smaller. In addition, water treatment operators may respond differently. On 01 August, the City of Toledo detected MC > 1 μg L^{-1} in the finished water, making high biomass a concern for all the water suppliers in the region. By September the MC concentrations in the lake had dropped substantially, even while the biomass had not. Providing a cyanotoxin map that looks much different from the biomass map, may allow for a more considered response by managers.

The stations used to develop the parameterizations are in the western half of the western basin of Lake Erie (west of 83°W). For a lake of this size, additional samples should be collected near the islands that mark the basin. Also, Sandusky Bay on the Ohio coast experiences cyanobacterial blooms dominated by *Planktothrix agardhii/suspensa* (Conroy et al., 2005; Davis et al., 2015b), which is the dominant MC-producer in the bay (Rinta-Kanto and Wilhelm, 2006; Davis et al., 2015b). An MC parameterization developed for *Microcystis* in Lake Erie is unlikely to be valid for *Planktothrix* in Sandusky Bay. The toxicity will vary between species, and the shape and behavior of the cells differs. *Microcystis* forms colonies and changes buoyancy, while *Planktothrix* forms trichomes and typically remains dispersed in the water column. Routine field calibration and validation are necessary to assure valid results across the lake or lakes.

In application, users need to consider sub-pixel variability. A pixel is an average of the radiance over the entire area, and a 300-m MERIS pixel covers an area greater than a football stadium. Concentrations can vary many-fold over the pixel (Kutser, 2009), although a method has recently been proposed to estimate sub-pixel variability for ocean color imagery (Salama and Su, 2010). With both sub-pixel variability and modeling uncertainties, each pixel should be expected to contain areas having concentrations several-fold greater than the pixel value.

6. Analytical uncertainties

Within a region, measurement of any constituent can vary considerably when different analytical methods and approaches are used, especially in the absence of certified reference materials, lack of standardized methods for sampling and processing, and

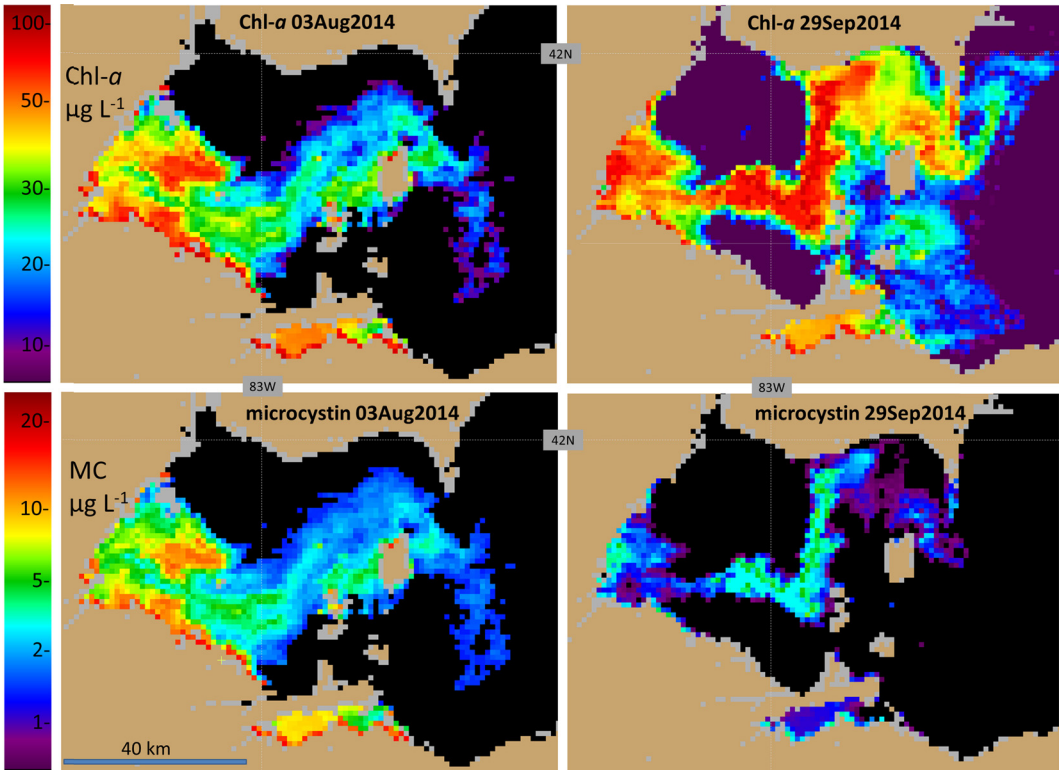

Fig. 7. Western Lake Erie, Chl-*a* and microcystin (MC). Top row: Chlorophyll surface concentration from Moderate Resolution Imaging Spectroradiometer (MODIS) data, calculated from the CI algorithm for 03 August and 29 September 2014; bottom row: microcystin concentration from the Chl-*a* using relationships derived from data for July 29 to 02 August and for 12–29 September. Clouds are gray, land is tan. Both are shown in log scale. Average measured MC concentration at stations in the southwestern lake was 6 μg L^{-1} (range 1.0 to 21 μg L^{-1}) between 29 July and 04 August and 1.6 μg L^{-1} (range 0.1 to 7) between 23 and 29 Sep.

differential response to analytical matrix effects that adversely impact the measurement of analyte concentration whether in the field, laboratory, or by remote sensing. When using multiple measurements, care must be exercised to adequately deal with measurement variation inclusive of methodological differences and to consider propagation of errors. These issues include cyanotoxins (Qian et al., 2015), but phytoplankton pigments such as Chl-*a* and PC are not exceptions (Jacobsen and Rai, 1990; Trees et al., 1985). Extraction methods for PC, without following strict and consistent protocols, can fail to extract over half of the pigment (Zimba, 2012). Even Chl-*a* metrics can vary substantially, particularly between different methods (Jacobsen and Rai, 1990). Some field programs use *in situ* or *in vivo* fluorometry to determine pigment concentrations. This approach will add additional uncertainty to the models, as intracellular and environmental factors alter *in vivo* fluorescence and the apparent amount of pigment per cell (Zamyadi et al., 2012).

ELISA is currently the most commonly used screening technique for cyanotoxins but the uncertainty associated with this method is rarely reported (Qian et al., 2015). There are at least 90 MC congeners reported in the literature (Chorus and Bartram, 1999) and multiple MC ELISAs with unique antibodies (including several commercial options) and therefore unique cross-reactivity (Weller, 2013). For a simple example, molar cross-reactivity for MCs-LR and -YR for the polyclonal MC ELISA reported by (Fischer et al., 2001) was 100 and 167% compared with cross-reactivity reported for the monoclonal ELISA reported by Zeck et al. (2001) of 100 and 120%, respectively. The difference in cross-reactivity can lead to the same answer if either an environmental sample was exclusively MC-LR or the sample had a quite different reported concentration such as 1 $\mu g\,L^{-1}$ of each of the MC congeners (e.g. total MC concentration of 2 $\mu g\,L^{-1}$). The differences can be magnified as the number of congeners present increases or the concentration of each congener increases. For example, changing the actual concentrations from 1 to 4 $\mu g\,L^{-1}$ for each congener in the previous example, the final concentration reported would equal 10.8 $\mu g\,L^{-1}$ (measured by Fischer et al., 2001) and 8.8 $\mu g\,L^{-1}$ measured by Zeck et al. (2001), a 20% difference. Using recreational World Health Organization (WHO) MC guidance values where 10 $\mu g\,L^{-1}$ triggered an action, only the Fischer et al. (2001) result would exceed this criterion. This demonstrates the need for known precision and accuracy based on certified reference materials and basic understanding of methodological differences especially at thresholds of concern.

It is therefore critical at a minimum to consider the implications of analytical errors and uncertainties in the laboratory methods on the model and the application of the model results. The introduction of substantive analytical error can occur in the absence of performance-based quality control approaches that correct for analyte recovery issues and matrix effects (such as standard addition or isotope dilution). The same field, sample processing, and laboratory methods should be applied to insure continuity of data interpretation to the ultimate users.

7. Parameterization of the dual model

Parameterization of the toxin-surrogate model can be solved in one of several ways, all with different confidence levels. If samples are rare, for example one or two per season, toxin maps should be avoided. They would give the impression of a knowledge that does not exist. Kudela et al. (2015) demonstrated this point effectively in Pinto Lake, California. They found shifts between non-toxic *Aphanizomenon*, and toxic *Microcystis*, with large variations in the relationship between MC and pigments. During the *Aphanizomenon* phase, the presence of PC was a poor indicator of MC, and failure to re-parameterize a surrogate model after the shifts between toxic and non-toxic species would lead to highly erroneous estimates of MC concentration or presence. Parameterization requires repeated samples and these samples must be taken at different pigment concentrations. The range of concentrations must exceed the uncertainties in the measurements based on sound statistical methods. With a measurement uncertainty of 30–50% in both pigment and toxin concentrations, the measured concentration range used for parameterization should exceed an order of magnitude in order to constrain the model uncertainty to useful levels. The relationship can be validated against data taken through the season and adjusted when it fails to meet the uncertainties needed for the application. With limited toxin data, only maps of pigment concentration should be produced. The analysis of water samples also needs confirmation of a cyanobacteria-dominated bloom in order to determine whether Chl-*a* or PC is the appropriate surrogate.

Remote sensing models generally lack evaluations of the parameterization (coefficients) for lakes. At present, the analytical and semi-analytical (ratio) models have parameterizations that appear to be applicable to new areas (Gons et al., 2008; Moses et al., 2012; Ruiz-Verdú et al., 2008). More investigation is needed into the stability of the coefficients when applied to satellite data, as well as to field measurements of reflectance (radiometry). The tuning of derivative algorithms has not been evaluated for global application, so this work needs to be conducted. If the derivatives use reflectance measurements, the parameterizations may be widely applicable to lakes covering a range of latitudes and sun angles, thereby improving their utility. In addition, for the CI method to be applied to cyanobacteria, fluorescing algae must be excluded from the parameterization. The same Chl-*a* concentration can occur with both a positive SS(681) in a bloom of fluorescing algae and a negative SS(681) in a cyanobacterial bloom. As a result, including fluorescing algae in a parameterization will introduce statistical leverage that will bias the relationship. These algae should be excluded, preferably by identifying only cyanobacteria from the SS(665) (Lunetta et al., 2015; Matthews et al., 2012).

Pigment is typically assumed to represent biomass (Ha et al., 2011; Kardinaal et al., 2007). Remote sensing does not detect volume; it detects the cross-sectional concentration of the absorption by pigments. If a cell has packaged more Chl-*a*, or has formed colonies (another kind of packaging), the relationship between absorption, pigment quantity, and biomass may also change. The temporal (or spatial) variation in the relationship between MCs and pigments can be caused by both the production of MC and pigments, and the packaging characteristics pigments in the cells. Understanding the pigment/biovolume variability will require field and laboratory studies of these characteristics to complement the remote sensing

8. Conclusions

Cyanotoxins cannot be directly measured with remote sensing. If the variability between cyanotoxins and a surrogate pigment is addressed, a dual-model strategy for remote sensing of these compounds is appropriate. A relationship between MC and either Chl-*a* or PC can remain constant for days to weeks within a lake. Over longer time intervals, a fixed parameterization may lead to large errors in estimated MC concentrations, therefore the parameterization should be validated every few weeks and adjusted as necessary. While PC is the better surrogate for mixed blooms, Chl-*a* is the superior surrogate for blooms dominated by cyanobacteria. Chl-*a* has a stronger optical signature than PC, it is more stable within the cells, the laboratory methods are

standardized, and it is more frequently measured. Satellite algorithms can quantify Chl-*a* in lakes, although the best accuracy requires MERIS or sensors with equivalent spectral bands. With MERIS, PC can also be quantified.

To obtain the surrogate pigments, derivative satellite algorithms have an advantage over analytical (and ratio) algorithms. Derivatives are insensitive to poor atmospheric correction and mild sun-glint, allow more robust and frequent application, as demonstrated by the increasing use of these methods in routine monitoring. They can address scum, a significant problem with analytical algorithms, which are based on the physics of light entering the water. On the other hand, analytical algorithms can retrieve PC. While derivatives appear able to identify PC, quantification still needs to be established. Analytical algorithms also have the capability of simultaneously retrieving several other characteristics of the water, such as backscatter, CDOM, and general pigment absorption, if these are of interest. Given that derivatives are based on the absorption characteristics of the pigments, radiative transfer modeling might identify analytical relationships between the derivatives and pigments that may enhance these algorithms.

The derivative algorithms still lack standardization of methods and calibration that allow universal evaluation of their parameterization. Extensive work has been done on parameterization and validation of remote sensing of oceanic Chl-*a*, which has led to an excellent understanding of the uncertainties in ocean Chl-*a* models. Lakes simply have not been studied in this way. New studies like GLOBOLAKES (NERC, 2015) and the Cyanobacterial Assessment Network (Schaeffer et al., 2015) may provide the comprehensive data sets of satellite and field pigments from many lakes that can be used to evaluate parameterizations. The ocean color community has also used field radiometry to parameterize relationships (O'Reilly et al., 2000) and then evaluated the satellite data with these methods. Lake studies have split on approaches. The analytical and semi-analytical methods have followed the ocean color lead, but the derivative methods have used mostly satellite to field matchups. Given the inherent spatial uncertainty in the distribution of blooms, and the potential issues with use of the appropriate satellite product, more attention should be made to the use of field measurements of reflectance to parameterize derivative-based pigment models (Tomlinson et al., 2016). This approach will help standardize processing of the satellite data to consistent reflectance-based products. Standardization is a factor in pigment and cyanotoxin measurement that will also require closer scrutiny. Propagation of known measurement error and uncertainty into the models will establish confidence levels for a variety of applications besides toxin maps.

Direct estimates of inter-annual variability of cyanotoxin concentration are probably an impossible task with satellite, because of the variability in the specific toxicity of the cells. Even estimation of pigment concentration requires care. Satellites see only the surface concentration (less than a meter), which is not total biomass. Determining average pigment concentrations will introduce biases into the resulting climate data unless the analysis compensates for winds through the use of compositing methods (Stumpf et al., 2012), phenological methods (Palmer et al., 2015b), or other modeling approaches.

Improving strategies for collecting pigment measurement with toxin measurement will allow a better understanding and use of remote sensing to inform monitoring of toxins in lakes. The remote sensing options will improve. The 2016 launch of the Ocean Land Colour Imager on Sentinel-3 will introduce a critical opportunity to address this need. OLCI replaces MERIS, with all the MERIS bands, and it will represent a future of data availability for most medium to large lakes around the world.

Acknowledgements

This work was partially funded by the NASA Public Health and Water Quality Program (NNH08ZDA001N) under contract NNH09AL53I, the NASA Ocean Biology and Biochemistry Programs under proposal 14-SMDUNSOL14-0001, the U.S. Geological Survey's Toxic Substances Hydrology Program, and the Environmental Protection Agency's Great Lake Research Initiative. This is NOAA GLERL publication number 1804. Steve Ruberg and the captains and crew of NOAA GLERL's research vessels provided invaluable support. Any use of trade, product, or firm names is for descriptive purposes only and does not imply endorsement by the U.S. Government. The paper benefitted from the insightful comments of the reviewers.

[SS]

References

Al-Ammar, R., Nabok, A., Hasim, A., Smith, T., 2013. Optical detection of microcystin produced by cyanobacteria. J. Phys.: Conf. Ser. 450 (1), 012006.

Babyak, M.A., 2004. What you see may not be what you get: a brief, nontechnical introduction to overfitting in regression-type models. Psychosom. Med. 66 (3), 411–421.

Becker, F., Choudhury, B.J., 1988. Relative sensitivity of normalized difference vegetation index (NDVI) and microwave polarization difference index (MPDI) for vegetation and desertification monitoring. Remote Sens. Environ. 24 (2), 297–311.

Behrenfeld, M.J., O'Malley, R.T., Siegel, D.A., McClain, C.R., Sarmiento, J.L., Feldman, G.C., Milligan, A.J., Falkowski, P.G., Letelier, R.M., Boss, E.S., 2006. Climate-driven trends in contemporary ocean productivity. Nature 444 (7120), 752–755.

Binding, C., Greenberg, T., Bukata, R., 2012. An analysis of MODIS-derived algal and mineral turbidity in Lake Erie. J. Great Lakes Res. 38 (1), 107–116.

Binding, C., Greenberg, T., Bukata, R., 2013. The MERIS maximum chlorophyll index; its merits and limitations for inland water algal bloom monitoring. J. Great Lakes Res. 39, 100–107.

Binding, C.E., Greenberg, T.A., Bukata, R.P., 2011. Time series analysis of algal blooms in Lake of the Woods using the MERIS maximum chlorophyll index. J. Plankton Res. 33 (12), 1847–1852.

Bricaud, A., Babin, M., Morel, A., Claustre, H., 1995. Variability in the chlorophyll-specific absorption coefficients of natural phytoplankton: analysis and parameterization. J. Geophys. Res. 100, 13,321–313,332.

Briand, E., Bormans, M., Quiblier, C., Salençon, M.J., Humbert, J.F., 2012. Evidence of the cost of the production of microcystins by *Microcystis aeruginosa* under differing light and nitrate environmental conditions. PLoS ONE 7 (1), e29981.

Carlson, R.E., 1977. A trophic state index for lakes. Limnol. Oceanogr. 22 (2), 361–369.

Carmichael, W.W., An, J., 1999. Using an enzyme linked immunosorbent assay (ELISA) and a protein phosphatase inhibition assay (PPIA) for the detection of microcystins and nodularins. Nat. Toxins 7 (6), 377–385.

Chaffin, J.D., Bridgeman, T.B., Heckathorn, S.A., Krause, A.E., 2012. Role of suspended sediments and mixing in reducing photoinhibition in the bloom-forming cyanobacterium Microcystis. J. Water Resour. Prot. 4 (12), 1029.

Chorus, I. (Ed.), 2005. Current Approaches to Cyanotoxin Risk Assessment, Risk Management and Regulations in Different Countries. Fed. Environmental Agency, ⟨http://www.umweltbundesamt.de/en/publications⟩

Chorus, E.I., Bartram, J., 1999. Toxic Cyanobacteria in Water: A Guide to Their Public Health Consequences, Monitoring and Management. E & FN Spon, London.

Chorus, I., Fastner, J., 2001. Recreational exposure to cyanotoxins. In: Cyanotoxins, Occurrence, Causes, ConsequencesSpringer, Heidelberg, pp. 190–199.

Conroy, J.D., Kane, D.D., Dolan, D.M., Edwards, W.J., Charlton, M.N., Culver, D.A., 2005. Temporal trends in Lake Erie plankton biomass: roles of external phosphorus loading and Dreissenid mussels. J. Great Lakes Res. 31, 89–110.

D'sa, E., Hu, C., Muller-Karger, F., Carder, K., 2002. Estimation of colored dissolved organic matter and salinity fields in case 2 waters using SeaWiFS: examples from Florida Bay and Florida Shelf. J. Earth Syst. Sci. 111 (3), 197–207.

Davis, T.W., Berry, D.L., Boyer, G.L., Gobler, C.J., 2009. The effects of temperature and nutrients on the growth and dynamics of toxic and non-toxic strains of Microcystis during cyanobacteria blooms. Harmful Algae 8 (5), 715–725.

Davis, T.W., Harke, M.J., Marcoval, M., Goleski, J., Orano-Dawson, C., Berry, D.L., Gobler, C.J., 2010. Effects of nitrogenous compounds and phosphorus on the growth of toxic and non-toxic strains of Microcystis during cyanobacterial blooms. Aquat. Microb. Ecol. 61 (2), 149.

Davis, T.W., Bullerjahn, G.S., Tuttle, T., McKay, R.M., Watson, S.B., 2015a. Effects of increasing nitrogen and phosphorus concentrations on the growth and toxicity of *Planktothrix* blooms in Sandusky Bay. Lake Erie. Environ. Sci. Technol. 49 (12), 7197–7207.

Davis, T.W., Watson, S.B., Roxmarynoycz, M.J., Ciborowski, J.J.H., McKey, R.M., Bullerahn, G.S., 2015b. Phylogenies of microcystin producing cyanobacteria in the lower Laurentian Great Lakes suggest extensive genetic connectivity. PLoS ONE 9, e10093.

De Marsac, N.T., 2003. Phycobiliproteins and phycobilisomes: the early observations. Photosynth. Res. 76 (1–3), 193–205.

Downing, J.A., Watson, S.B., McCauley, E., 2001. Predicting cyanobacteria dominance in lakes. Can. J. Fish. Aquat. Sci. 58 (10), 1905–1908.

Duan, H., Ma, R., Zhang, Y., Loiselle, S.A., 2014. Are algal blooms occurring later in Lake Taihu? Climate local effects outcompete mitigation prevention. J. Plankton Res. 36 (3), 866–871.

Falconer, I.R., Humpage, A.R., 2005. Health risk assessment of cyanobacterial (blue-green algal) toxins in drinking water. Int. J. Environ. Res. Public Health 2 (1), 43–50.

Fastner, J., Wirsing, B., Wiedner, C., Heinze, R., Neumann, U., Chorus, I., 2001. Microcystins and hepatocyte toxicity. In: Cyanotoxins, Occurrence, Causes, ConsequencesHeidelberg, Springer, pp. 22–37.

Fischer, W.J., Garthwaite, I., Miles, C.O., Ross, K.M., Aggen, J.B., Chamberlin, A.R., Towers, N.R., Dietrich, D.R., 2001. Congener-independent immunoassay for microcystins and nodularins. Environ. Sci. Technol. 35 (24), 4849–4856.

Gilerson, A.A., Gitelson, A.A., Zhou, J., Gurlin, D., Moses, W., Ioannou, I., Ahmed, S.A., 2010. Algorithms for remote estimation of chlorophyll-*a* in coastal and inland waters using red and near infrared bands. Opt. Express 18 (23), 24109–24125.

Gitelson, A., 1992. The peak near 700 nm on radiance spectra of algae and water: relationships of its magnitude and position with chlorophyll concentration. Int. J. Remote Sens. 13 (17), 3367–3373.

Gobler, C.J., Burkholder, J.M., Davis, T.W., Harke, M.J., Johengen, T., Stow, C.A., van de Waal, D.B., 2016. The dual role of nitrogen supply in controlling the growth and toxicity of cyanobacterial blooms. Harmful Algae 54, 87–97.

Gómez, J.A.D., Alonso, C.A., García, A.A., 2011. Remote sensing as a tool for monitoring water quality parameters for Mediterranean Lakes of European Union water framework directive (WFD) and as a system of surveillance of cyanobacterial harmful algae blooms (SCyanoHABs). Environ. Monit. Assess. 181 (1–4), 317–334.

Gons, H.J., Auer, M.T., Effler, S.W., 2008. MERIS satellite chlorophyll mapping of oligotrophic and eutrophic waters in the Laurentian Great Lakes. Remote Sens. Environ. 112 (11), 4098–4106.

Gordon, H., Morel, A., 1983. Remote Assessment of Ocean Color for Interpretation of Satellite Visible Imagery: A Review. Lecture Notes on Coastal and Estuarine Studies, Springer-Verlag, Berlin Heidelberg, pp. 4.

Gower, J., King, S., Borstad, G., Brown, L., 2005. Detection of intense plankton blooms using the 709 nm band of the MERIS imaging spectrometer. Int. J. Remote Sens. 26 (9), 2005–2012.

Graham, J.L., Loftin, K.A., Kamman, N., 2009. Monitoring recreational freshwaters. Lakelines 29, 18–24.

Graham, J.L., Loftin, K.A., Meyer, M.T., Ziegler, A.C., 2010. Cyanotoxin mixtures and taste-and-odor compounds in cyanobacterial blooms from the Midwestern United States. Environ. Sci. Technol. 44 (19), 7361–7368.

Ha, J.H., Hidaka, T., Tsuno, H., 2011. Analysis of factors affecting the ratio of microcystin to chlorophyll-*a* in cyanobacterial blooms using real-time polymerase chain reaction. Environ. Toxicol. 26 (1), 21–28.

Hu, C., Lee, Z., Ma, R., Yu, K., Li, D., Shang, S., 2010. Moderate Resolution Imaging spectroradiometer (MODIS) observations of cyanobacteria blooms in Taihu Lake, China. Geophys. Res.: Oceans 115 (C04002), http://dx.doi.org/10.1029/2009JC005511.

Hu, C., Lee, Z., Franz, B., 2012. Chlorophyll algorithms for oligotrophic oceans: a novel approach based on three-band reflectance difference. J. Geophys. Res.: Oceans 117 (C01011), http://dx.doi.org/10.1029/2011JC007395.

Hunter, P., Tyler, A., Willby, N., Gilvear, D., 2008. The spatial dynamics of vertical migration by *Microcystis aeruginosa* in a eutrophic shallow lake: a case study using high spatial resolution time-series airborne remote sensing. Limnol. Oceanogr. 53 (6), 2391–2406.

Ibelings, B.W., Backer, L.C., Kardinaal, W.E.A., Chorus, I., 2014. Current approaches to cyanotoxin risk assessment and risk management around the globe. Harmful Algae 40, 63–74.

Jacobsen, T.R., Rai, H., 1990. Comparison of spectrophotometric, fluorometric and high performance liquid chromatography methods for determination of chlorophyll *a* in aquatic samples: effects of solvent and extraction procedures. Internationale Revue der gesamten Hydrobiologie und Hydrographie 75 (2), 207–217.

Kahru, M., Elmgren, R., 2014. Multidecadal time series of satellite-detected accumulations of cyanobacteria in the Baltic Sea. Biogeosciences 11 (13), 3619–3633.

Kardinaal, W.E.A., Tonk, L., Janse, I., Hol, S., Slot, P., Huisman, J., Visser, P.M., 2007. Competition for light between toxic and nontoxic strains of the harmful cyanobacterium Microcystis. Appl. Environ. Microbiol. 73 (9), 2939–2946.

Kardinaal, W.E.A., Visser, P.M., 2005. Dynamics of Cyanobacterial Toxins. Harmful Cyanobacteria Aquatic Ecology Series, Springer, Dordrecht, the Netherlands, , pp. 41–64.

Kasinak, J.-M.E., Holt, B.M., Chislock, M.F., Wilson, A.E., 2015. Benchtop fluorometry of phycocyanin as a rapid approach for estimating cyanobacterial biovolume. J. Plankton Res. 37 (1), 248–257.

Kirk, J.T., 1994. Light and Photosynthesis in Aquatic Ecosystems. Cambridge University Press, New York.

Kudela, R.M., Palacios, S.L., Austerberry, D.C., Accorsi, E.K., Guild, L.S., Torres-Perez, J., 2015. Application of hyperspectral remote sensing to cyanobacterial blooms in inland waters. Remote Sens. Environ. 167, 196–205.

Kutser, T., 2009. Passive optical remote sensing of cyanobacteria and other intense phytoplankton blooms in coastal and inland waters. Int. J. Remote Sens. 30 (17), 4401–4425.

Lawrenz, E., Fedewa, E.J., Richardson, T.L., 2011. Extraction protocols for the quantification of phycobilins in aqueous phytoplankton extracts. J. Appl. Phycol. 23 (5), 865–871.

Letelier, R.M., Abbott, M.R., 1996. An analysis of chlorophyll fluorescence algorithms for the Moderate Resolution Imaging Spectrometer (MODIS). Remote Sens. Environ. 58 (2), 215–223.

Lunetta, R.S., Schaeffer, B.A., Stumpf, R.P., Keith, D., Jacobs, S.A., Murphy, M.S., 2015. Evaluation of cyanobacteria cell count detection derived from MERIS imagery across the eastern USA. Remote Sens. Environ. 157, 24–34.

Lyck, S., 2004. Simultaneous changes in cell quotas of microcystin, chlorophyll *a*, protein and carbohydrate during different growth phases of a batch culture experiment with *Microcystis aeruginosa*. J. Plankton Res. 26 (7), 727–736.

Matthews, M.W., 2011. A current review of empirical procedures of remote sensing in inland and near-coastal transitional waters. Int. J. Remote Sens. 32 (21), 6855–6899.

Matthews, M.W., 2014. Eutrophication and cyanobacterial blooms in South African inland waters: 10years of MERIS observations. Remote Sens. Environ. 155, 161–177.

Matthews, M.W., Bernard, S., Robertson, L., 2012. An algorithm for detecting trophic status (chlorophyll-*a*), cyanobacterial-dominance, surface scums and floating vegetation in inland and coastal waters. Remote Sens. Environ. 124, 637–652.

Matthews, M.W., Odermatt, D., 2015. Improved algorithm for routine monitoring of cyanobacteria and eutrophication in inland and near-coastal waters. Remote Sens. Environ. 156, 374–382.

Mishra, S., Mishra, D.R., Schluchter, W.M., 2009. A novel algorithm for predicting phycocyanin concentrations in cyanobacteria: a proximal hyperspectral remote sensing approach. Remote Sens. 1 (4), 758–775.

Mishra, S., Mishra, D.R., Lee, Z., Tucker, C.S., 2013. Quantifying cyanobacterial phycocyanin concentration in turbid productive waters: a quasi-analytical approach. Remote Sens. Environ. 133, 141–151.

Monchamp, M.-E., Pick, F.R., Beisner, B.E., Maranger, R., 2014. Nitrogen Forms Influence Microcystin Concentration and Composition via Changes in Cyanobacterial Community Structure. PLoS ONE 9 (1), e85573, http://dx.doi.org/10.1371/journal.pone.0085573.

Moradi, M., 2014. Comparison of the efficacy of MODIS and MERIS data for detecting cyanobacterial blooms in the southern Caspian Sea. Mar. Pollut. Bull. 87 (1), 311–322.

Moses, W.J., Gitelson, A.A., Berdnikov, S., Saprygin, V., Povazhnyi, V., 2012. Operational MERIS-based NIR-red algorithms for estimating chlorophyll-*a* concentrations in coastal waters—the Azov Sea case study. Remote Sens. Environ. 121, 118–124.

NERC, 2015. Globolakes ⟨http://www.globolakes.ac.uk/⟩ (accessed October 15, 2015).

Ohio EPA, 2015. Harmful Algal Blooms ⟨http://epa.ohio.gov/ddagw/HAB.aspx⟩ (accessed Oct 15, 2015).

Oliver, R.L., Hamilton, D.P., Brookes, J.D., Ganf, G.G., 2012. Physiology, Blooms and Prediction of Planktonic Cyanobacteria, Chapter 6. In: Whitton, B.A. (Ed.), Ecology of Cyanobacteria II: Their Diversity in Space and Time. Springer Science & Business Media, Netherlands.

Olmanson, L.G., Brezonik, P.L., Bauer, M.E., 2011. Evaluation of medium to low resolution satellite imagery for regional lake water quality assessments. Water Resour. Res. 47 (9), http://dx.doi.org/10.1029/2011WR011005.

O'Neil, J., Davis, T.W., Burford, M.A., Gobler, C., 2012. The rise of harmful cyanobacteria blooms: the potential roles of eutrophication and climate change. Harmful Algae 14, 313–334.

O'Reilly, J.E., Maritorena, S., Siegel, D.A., O'Brien, M.C., Toole, D., Mitchell, B.G., Kahru, M., Chavez, F.P., Strutton, P., Cota, G.F., 2000. Ocean color chlorophyll *a* algorithms for SeaWiFS, OC2, and OC4: Version 4In: SeaWiFS Postlaunch Calibration and Validation Analyses, Part 3, pp. 9–23.

Orr, P.T., Jones, G.J., 1998. Relationship between microcystin production and cell division rates in nitrogen-limited *Microcystis aeruginosa* cultures. Limnol. Oceanogr. 43 (7), 1604–1614.

Palmer, S.C., Hunter, P.D., Lankester, T., Hubbard, S., Spyrakos, E., Tyler, A.N., et al., 2015a. Validation of Envisat MERIS algorithms for chlorophyll retrieval in a large, turbid and optically-complex shallow lake. Remote Sens. Environ. 157, 158–169.

Palmer, S., Odermatt, D., Hunter, P., Brockmann, C., Presing, M., Balzter, H., Tóth, V., 2015b. Satellite remote sensing of phytoplankton phenology in Lake Balaton using 10 years of MERIS observations. Remote Sens. Environ. 158, 441–452.

Pearson, L.A., Dittmann, E., Mazmouz, R., Ongley, S.E., D'Agostino, P.M., Neilan, B.A., 2016. The genetics, biosynthesis and regulation of toxic specialised metabolites in cyanobacteria. Harmful Algae 54, 98–111.

Philpot, W.D., 1991. The derivative ratio algorithm: avoiding atmospheric effects in remote sensing. IEEE Trans. Geosci. Remote Sens. 29 (3), 350–357.

Qi, L., Hu, C., Duan, H., Cannizzaro, J., Ma, R., 2014. A novel MERIS algorithm to derive cyanobacterial phycocyanin pigment concentrations in a eutrophic lake: theoretical basis and practical considerations. Remote Sens. Environ. 154, 298–317.

Qian, S.S., Chaffin, J.D., DuFour, M.R., Sherman, J.J., Golnick, P.P., Collier, C.D., Nummer, S.A., Margida, M.G., 2015. Quantifying and reducing uncertainty in estimated microcystin concentrations from the ELISA method. Environ. Sci. Technol. 49 (24), 14221–14229.

Raven, J., 1984. A cost-benefit analysis of photon absorption by photosynthetic unicells. New Phytol. 98 (4), 593–625.

Reuter, W., Müller, C., 1993. New trends in photobiology: adaptation of the photosynthetic apparatus of cyanobacteria to light and CO2. J. Photochem. Photobiol, B: Biol. 21 (1), 3–27.

Rinta-Kanto, J.M., Wilhelm, S.W., 2006. Diversity of microcystin producting cyanobacteria in spatially isolated regions of Lake Erie. Appl. Environ. Microbiol. 72, 5083–5085.
Ruiz-Verdú, A., Simis, S.G., de Hoyos, C., Gons, H.J., Peña-Martínez, R., 2008. An evaluation of algorithms for the remote sensing of cyanobacterial biomass. Remote Sens. Environ. 112 (11), 3996–4008.
Salama, M.S., Su, Z., 2010. Bayesian model for matching the radiometric measurements of aerospace and field ocean color sensors. Sensors 10 (8), 7561–7575.
Salisbury, J., Vandemark, D., Campbell, J., Hunt, C., Wisser, D., Reul, N., Chapron, B., 2011. Spatial and temporal coherence between Amazon River discharge, salinity, and light absorption by colored organic carbon in western tropical Atlantic surface waters. J. Geophys. Res. Oceans (1978–2012) 116 (C00H02), http://dx.doi.org/10.1029/2011JC006989.
Sass, G., Creed, I., Bayley, S., Devito, K., 2007. Understanding variation in trophic status of lakes on the Boreal Plain: a 20 year retrospective using Landsat TM imagery. Remote Sens. Environ. 109 (2), 127–141.
Schaeffer, B.A., Loftin, K., Stumpf, R.P., Werdell, P.J., 2015. Agencies collaborate, develop a cyanobacteria assessment network. Eos 96,, http://dx.doi.org/10.1029/2015EO038809, Published on 10 November 2015.
Seppälä, J., Ylöstalo, P., Kaitala, S., Hällfors, S., Raateoja, M., Maunula, P., 2007. Ship-of-opportunity based phycocyanin fluorescence monitoring of the filamentous cyanobacteria bloom dynamics in the Baltic Sea. Estuarine Coastal Shelf Sci. 73 (3), 489–500.
Shi, K., Zhang, Y., Xu, H., Zhu, G., Qin, B., Huang, C., Liu, X., Zhou, Y., Heng, L., 2015. Long-term satellite observations of microcystin concentrations in Lake Taihu during cyanobacterial bloom periods. Environ. Sci. Technol. 49 (11), 6448–6456.
Simis, S.G., Peters, S.W., Gons, H.J., 2005. Remote sensing of the cyanobacterial pigment phycocyanin in turbid inland water. Limnol. Oceanogr. 50 (1), 237–245.
Simis, S.G., Ruiz-Verdú, A., Domínguez-Gómez, J.A., Peña-Martinez, R., Peters, S.W., Gons, H.J., 2007. Influence of phytoplankton pigment composition on remote sensing of cyanobacterial biomass. Remote Sens. Environ. 106 (4), 414–427.
Stumpf, R.P., Tyler, M.A., 1988. Satellite detection of bloom and pigment distributions in estuaries. Remote Sens. Environ. 24 (3), 385–404.
Stumpf, R.P., Werdell, P.J., 2010. Adjustment of ocean color sensor calibration through multi-band statistics. Opt. Express 18 (2), 401–412.
Stumpf, R.P., Wynne, T.T., Baker, D.B., Fahnenstiel, G.L., 2012. Interannual variability of cyanobacterial blooms in Lake Erie. PLoS ONE 7 (8), e42444.
Trees, C.C., Kennicutt, M.C., Brooks, J.M., 1985. Errors associated with the standard fluorimetric determination of chlorophylls and phaeopigments. Mar. Chem. 17 (1), 1–12.
Tomlinson, M.C., Stumpf, R.P., Wynne, T.T., 2015. Relating chlorophyll from cyanobacteria-dominated inland waters to a MERIS bloom index. Remote Sens. Lett. 7 (2), 141–149.
Visser, P.M., Ibelings, B.W., Mur, L.R., Walsby, A.E., 2005. The ecophysiology of the harmful cyanobacterium microcystis. In: Huisman, J., Matthijs, H.C.P., Visser, P.M. (Eds.), Harmful Cyanobacteria. Springer, AA Dordrecht, pp. 109–142.
Wang, M., Shi, W., 2007. The NIR-SWIR combined atmospheric correction approach for MODIS ocean color data processing. Opt. Express 15 (24), 15722–15733.
Wehr, J.D., Sheath, R.G., 2003. Freshwater Algae of North America: Ecology and Classification. Elsevier, London.
Weller, M.G., 2013. Immunoassays and biosensors for the detection of cyanobacterial toxins in water. Sensors 13 (11), 15085–15112.
Wynne, T., Stumpf, R., Tomlinson, M., Warner, R., Tester, P., Dyble, J., Fahnenstiel, G., 2008. Relating spectral shape to cyanobacterial blooms in the Laurentian Great Lakes. Int. J. Remote Sens. 29 (12), 3665–3672.
Wynne, T.T., Stumpf, R.P., 2015. Spatial and temporal patterns in the seasonal distribution of toxic cyanobacteria in Western Lake Erie from 2002–2014. Toxins 7 (5), 1649–1663.
Wynne, T.T., Stumpf, R.P., Tomlinson, M.C., Dyble, J., 2010. Characterizing a cyanobacterial bloom in western Lake Erie using satellite imagery and meteorological data. Limnol. Oceanogr. 55 (5), 2025–2036.
Wynne, T.T., Stumpf, R.P., Briggs, T.O., 2013a. Comparing MODIS and MERIS spectral shapes for cyanobacterial bloom detection. Int. J. Remote Sens. 34 (19), 6668–6678.
Wynne, T.T., Stumpf, R.P., Tomlinson, M.C., Fahnenstiel, G.L., Dyble, J., Schwab, D.J., Joshi, S.J., 2013b. Evolution of a cyanobacterial bloom forecast system in western Lake Erie: development and initial evaluation. J. Great Lakes Res. 39, 90–99.
Zamyadi, A., McQuaid, N., Dorner, S., Bird, D.F., Burch, M., Baker, P., Hobson, P., Prevost, M., 2012. Cyanobacterial detection using in vivo fluorescence probes: managing interferences for improved decision-making. J. Am. Water Works Assoc. 104 (8), 37.
Zeck, A., Weller, M.G., Bursill, D., Niessner, R., 2001. Generic microcystin immunoassay based on monoclonal antibodies against adda. Analyst 126 (11), 2002–2007.
Zhang, Y., Duan, H., 2008. Cyanobacteria bloom detection and monitoring from satellite observations in the coastal region of Finland. J. Lake Sci. 20 (2), 167–172.
Zimba, P.V., 2012. An improved phycobilin extraction method. Harmful Algae 17, 35–39.